First Quantization Matrix Estimation From Double Compressed JPEG Images

Fausto Galvan, Giovanni Puglisi, Arcangelo Ranieri Bruna, and Sebastiano Battiato, *Senior Member, IEEE*

***Abstract*— One of the most common problems in the image forensics field is the reconstruction of the history of an image or a video. The data related to the characteristics of the camera that carried out the shooting, together with the reconstruction of the (possible) further processing, allow us to have some useful hints about the originality of the visual document under analysis. For example, if an image has been subjected to more than one JPEG compression, we can state that the considered image is not the exact bitstream generated by the camera at the time of shooting. It is then useful to estimate the quantization steps of the first compression, which, in case of JPEG images edited and then saved again in the same format, are no more available in the embedded metadata. In this paper, we present a novel algorithm to achieve this goal in case of double JPEG compressed images. The proposed approach copes with the case when the second quantization step is lower than the first one, exploiting the effects of successive quantizations followed by dequantizations. To improve the results of the estimation, a proper filtering strategy together with a function devoted to find the first quantization step, have been designed. Experimental results and comparisons with the state-of-the-art methods, confirm the effectiveness of the proposed approach.**

***Index Terms*— Double JPEG compression, forgery identification, digital tampering, image forensics, DCT coefficient analysis.**

I. Introduction

IN A digital investigation that includes JPEG images (the most widely used format on the network [1] and employed by most of cameras [2]) as evidences, the classes of problems that we have to deal with, are essentially two. The former concerns the authenticity of the visual document under analysis: if we are able to prove that it is not original and it has been changed with the insertion (or removal) of some details, we must then identify where the non-original parts are located. The latter is related to the retrieval of the device that generated the image under analysis. About the possibility to discover image manipulations in JPEG images, many approaches can be found in literature, as summarized in [3] and [4]. A first group of works (JPEG blocking artifacts analysis [5], [6], hash functions [7], JPEG headers analysis [2], thumbnails analysis [8], Exif analysis [9], etc.) proposes methods that seek the traces of the forgeries in the structure of the image or in its metadata. In [10] some methods based on PRNU (Photo Response Non-Uniformity) are exposed and tested. This kind of pattern characterizes, and allows to distinguish, every single camera sensor. Other approaches, as described in [11] and [12], take care of analyzing the statistical distribution of the values assumed by the DCT coefficients. In this regard, as reported in [13] and [14], by checking the related histogram, it is possible to determine whether the image was doubly JPEG compressed. In [15] a Bayesian approach calculates the probability for each block of the image of being subjected to double quantization, and uses the results of such control, together with a SVM classifier, to identify the tampered areas. SVM is also exploited in [16], where a Markov random process is employed to model the differences between the images, and in [17], where the tampering detection method is based on a periodic function detection strategy. In [18] the authors suggest a method that assess whether an image has been compressed twice with the same quantization table. In [19] the recompression with the same quantization table is detected in case of a copy-paste operation, observing that in this scenario there is a high probability that the grid of the pasted part is not aligned with the existing one.

The ability to roughly reconstruct the quantization table used by the device during acquisition, is crucial in almost all problems stated above. Specifically, this information discriminates which spatial regions are associated with the same (original) quantization table, evidencing as corrupted the ones that show different data. Retrieving some (even not all) components of the first quantization matrix, allow to look for the model of devices employing the same quantization tables identified before. For this purpose a collection of quantization tables together with their corresponding camera, like the one exposed in [2], has to be collected. The information about the first quantization matrix is also important for steganalysis, as reported in [20].

To retrieve the first quantization matrix, in [14] the authors expose some ideas based on the behavior of normalized histograms. They also focused on a method that uses a Neural Network as a classifier. Their approach, however, does not work for medium and high frequencies, and it has been proved only for a specific subset of the AC terms. The works in [21] and [22] also estimate the first quantization step, but only to locate forgeries and without providing exhaustive results related to its estimation. The method in [22] explores two types of traces left by tampering in doubly-compressed

Manuscript received November 8, 2013; revised March 6, 2014 and May 29, 2014; accepted June 2, 2014. Date of publication June 12, 2014; date of current version July 11, 2014. The associate editor coordinating the review of this manuscript and approving it for publication was Prof. Chiou-Ting Hsu.

F. Galvan is with the University of Udine, Udine 33100, Italy (e-mail: fausto.galvan@uniud.it).

G. Puglisi, A. R. Bruna, and S. Battiato are with the Department of Mathematics and Computer Science, University of Catania, Catania 95124, Italy (e-mail: puglisi@dmi.unict.it; arcbru@gmail.com; battiato@dmi.unict.it).

Color versions of one or more of the figures in this paper are available online at http://ieeexplore.ieee.org.

Digital Object Identifier 10.1109/TIFS.2014.2330312

JPEG images: aligned and non-aligned. These two scenarios arise depending if the DCT grid of the portion of image pasted in a splicing or cloning operation is (or not) aligned with the one of the original image. In [22] authors build a likelihood map to find the regions that have undergone to a double JPEG compression. Among the parameters required to correctly identify this likelihood map and modeling the doubly compressed regions, the quantization step of the primary compression is crucial. The authors estimate this parameter by using the expectation-maximization (EM) algorithm over a set of candidates. This procedure is replicated for each entry of the first-compression matrix. In [23] a method for the estimation of JPEG compression history is proposed but it works only for JPEG images converted into a lossless format. Frequency domain has been exploited in [24] where the authors introduce a technique based on the study of the frequency response to identify the first quantization step in precompressed raw images, and also in doubly compressed JPEG images, obtaining less reliable results. In [25] the author, to estimate q_1,[1] proposes to carry out a third quantization and then computes the error between the DCT coefficients before and after this step; by varying the quantization step of the third compression applied to the image, is possible to detect two minima in correspondence of q_1 and q_2. Although the paper was not strictly dedicated to recovery the quantization steps of the first quantization matrix, but to the identification of the tampered regions (the so called "ghosts"), the presented approach (a third quantization of the image) partially inspired our error function (4), which indeed is based upon two quantizations of the image under analysis. Later, in [26], an automated method that uses the approach in [25] is proposed.

In this paper we focus on the determination of the first quantization step in doubly compressed JPEG images, assuming that its value is higher (in JPEG compression standard, the bigger the quantization step is, the lower the quality of the image is) than the second one. It is worth noting that also [25] deals with a similar condition. Moreover, although other methods ([22], [27], [28]) have been designed to work also in the remaining case ($q_1 \leq q_2$), they actually obtain reliable results (i.e., a far lower error) only when $q_1 > q_2$. Therefore, starting from the assumption that the image has been doubly JPEG compressed (it can be previously verified with a method like the one exposed in [13]), the proposed approach analyzes histograms of its requantized DCT coefficients, exploiting their peculiarities. Specifically, when the second compression is lighter than the first one, retrieving the first quantization step is often possible. This can be done taking advantage of some interesting properties of integer numbers, that occurs whenever they are quantized (that means rounded) more than once.

The main novelties of the proposed approach are related to the filtering strategy, adopted to reduce the amount of noise in the input data (DCT histograms), and on the design of a novel function with a satisfactory q_1-localization property.

Indeed, although the proof of concept of the proposed approach has been partially presented in [29], in the present work we have improved that algorithm, including a modified version of the histogram filtering strategy proposed in [30]. Specifically, a novel filtering has been introduced to deal with what we called "split noise". Moreover, a whole section has been introduced to deeply study the impact of the involved parameters improving the selection of the candidates. Tests have been performed on different datasets with a certain variability in terms of image content. Finally, additional comparisons with state-of-the-art approaches are now provided.

The paper is structured as follows: in Section II JPEG compression algorithm, together with some properties of double compressed images are reviewed. Section III presents the proposed approach, providing the involved details related to the histogram filtering, the proposed function, the selection of the candidates and the final q_1 selection based on the histogram values. In Section IV the effectiveness of the proposed solution is reported, considering real data (double JPEG compressed images). Finally, in Section V we report conclusions and our prospects for future work in this field.

II. Scientific Background

The first step in the JPEG compression engine [32] consists in a partition of the input image into 8×8 pixels non-overlapping blocks (for both luminance and chrominance channels). A DCT transform is then applied to each block; next a dead-zone quantization is employed just using for each DCT coefficient a corresponding integer value belonging to a 8×8 quantization matrix [33]. The error introduced in this stage is called quantization error, and it is the main cause of information loss for JPEG compressed images. The quantized coefficients obtained just rounding the results of the ratio between the original DCT coefficients and the corresponding quantization steps are then transformed into a data stream by mean of a classic entropy coding (i.e., run length/variable length). Coding parameters and other metadata are usually inserted into the JPEG file header to allow a proper decoding. If an image has been JPEG compressed twice (e.g., after having visualized the image, introduced some malicious manipulation and saved it again) the last quantization steps are available, whereas the original (initial) ones are lost. It is worth noting that in forensics application, this information could be fundamental to assess the integrity of the input image or to reconstruct some information about the embedded manipulation [2]. The insertion of some kind of tampering requires the decompression of the image file, followed by a second JPEG compression after the forgery. During JPEG decompression, the pipeline of the image compression is retraced conversely. The compressed image is then entropy decoded (the quantized coefficients are recovered exactly), and the resulting coefficients are then multiplied by the same 8×8 quantization matrix to obtain the de-quantized coefficients. After that, the Inverse DCT (IDCT) is performed, bringing the coefficients from the frequency domain back into the spatial domain, to get the visible image. For this aim, the resulting real values will be rounded and truncated to the nearest integers in the range of [0; 255], generating other two errors, namely respectively rounding and truncation error. In addition, and for

[1]From here on q_1 and q_2 will indicate respectively the quantization steps of first and second quantization for a generic frequency in the DCT domain.

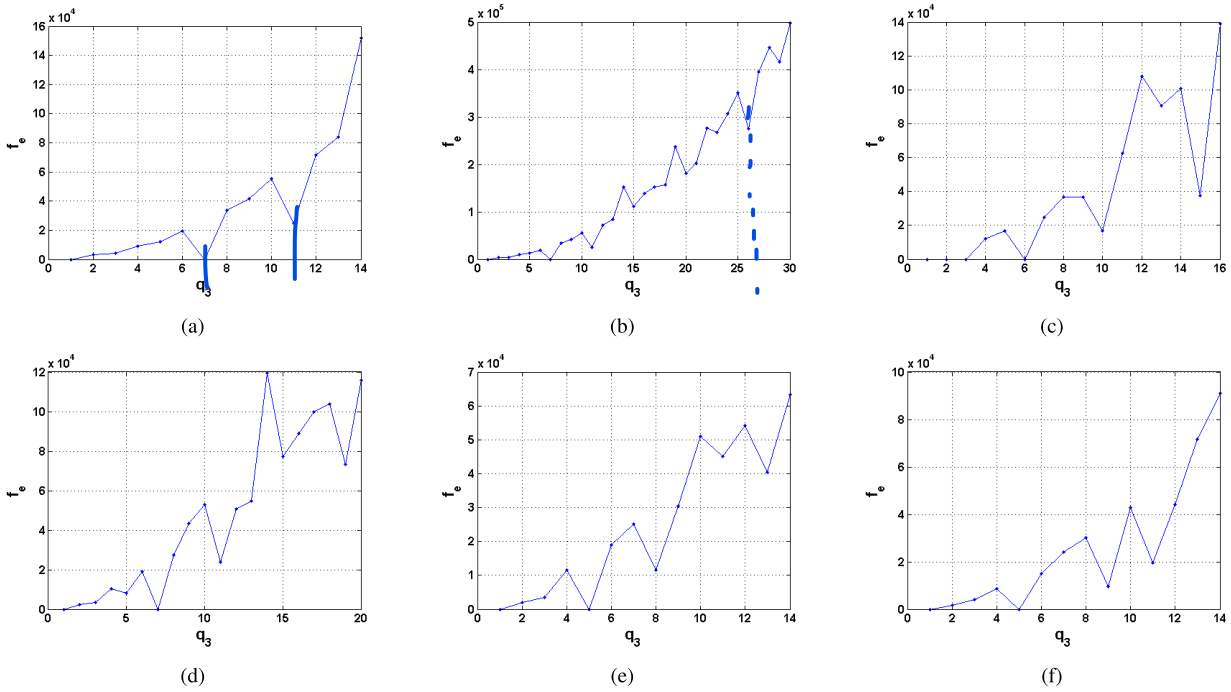

Fig. 1. In the upper row three examples of the error function values (2) for an image of the same dataset used in [31], with respect to q_3 for the DC term: (a) $q_1 = 11$, $q_2 = 7$ and $q_3 \in \{1, 2, \ldots, 14\}$; (b) $q_1 = 11$, $q_2 = 7$ and $q_3 \in \{1, 2, \ldots, 30\}$; (c) $q_1 = 10$, $q_2 = 6$ and $q_3 \in \{1, 2, \ldots, 16\}$. In the lower row three examples of the error function values (2) for the same image, with respect to q_3 for some AC term: (d) (1,0) term, $q_1 = 11$, $q_2 = 7$ and $q_3 \in \{1, 2, \ldots, 20\}$; (e) (2,0) term, $q_1 = 8$, $q_2 = 5$ and $q_3 \in \{1, 2, \ldots, 14\}$; (f) (3,0) term, $q_1 = 9$, $q_2 = 5$ and $q_3 \in \{1, 2, \ldots, 14\}$.

completeness of exposition, we must also considerate the error occurring during the conversion between RGB and YCbCr color spaces, and viceversa.

In the following analysis, only 8-bit grayscale images are considered. For sake of simplicity, considering a single DCT coefficient c and the related quantization steps q_1 (first quantization) and q_2 (second quantization), the value of each coefficient after a double compression can be modeled as:

$$c_{DQ} = \left[\left(\left[\frac{c}{q_1} \right] q_1 + e \right) \frac{1}{q_2} \right] \tag{1}$$

where $[.]$ denotes the rounding function and e is the error introduced by several operations, such as color conversions (YCbCr to RGB and vice versa), rounding and truncation of the values to eight bit integers, etc. It is important to note that the errors above can be due to some processing in different domains (e.g., spatial domain). In any case e is the effect of such errors in the DCT coefficients. Note that the factor e, often omitted in previous published works ([13], [25], [27]), if not properly managed, can limit the effectiveness of any related methodology.

To infer the value of q_1, Farid [25] suggests to perform a further compression with a novel quantization step q_3 (in a proper range) and to evaluate an error function defined as follows:

$$f_e(c, q_1, q_2, q_3) = \left| \left[\left[\left[\frac{c}{q_1} \right] \frac{q_1}{q_2} \right] \frac{q_2}{q_3} \right] q_3 - \left[\left[\frac{c}{q_1} \right] \frac{q_1}{q_2} \right] q_2 \right| \tag{2}$$

It is worth noting that the error e of Eq. (1) has not been considered in Eq. (2). The typical outcome of Eq. (2) considering, e.g., the DC term when $q_1 = 11$ and $q_2 = 7$ is reported in Fig. 1(a). This specific case (both quantization steps are prime numbers) allows obtaining interesting results: both q_1 and q_2 can be easily found, since they correspond to the two evident local minima. Hence, the first quantization step q_1 can be retrieved (q_2, as mentioned before, is already available). Unfortunately, in real cases, the original quantization step cannot be easily inferred as proved by considering the following cases:

- Range extension: taking into account the quantization steps used before ($q_1 = 11$, $q_2 = 7$) and the same input image, but varying $q_3 \in \{1, 2, \ldots, 30\}$, the outcome is more complex to analyze than before. A strong indication of a "wrong" local minimum can be found in 26 (see Fig. 1(b)).
- Different quantization steps: with the same input image and $q_3 \in \{1, 2, \ldots, 16\}$, but considering $q_1 = 10$ and $q_2 = 6$, the outcome reported in Fig. 1(c) is obtained. Without additional information about the input image, a wrong estimation ($q_1 = 15$) could be performed.
- Different AC frequencies: with the same input image but in different position and for many combinations of quantization steps, we could obtain again wrong estimations ($q_1 = 19$ instead of 11 in Fig. 1(d), $q_1 = 13$ instead of 8 in Fig. 1(e) and $q_1 = 11$ instead of 9 in Fig. 1(f)).

When $q_3 = q_2$, the error function (2) is equal to 0. This motivates the absolute minima found in the previous examples. Of course, Eq. (2) allows estimating q_2, but this information is not useful since q_2 is already known from the bitstream.

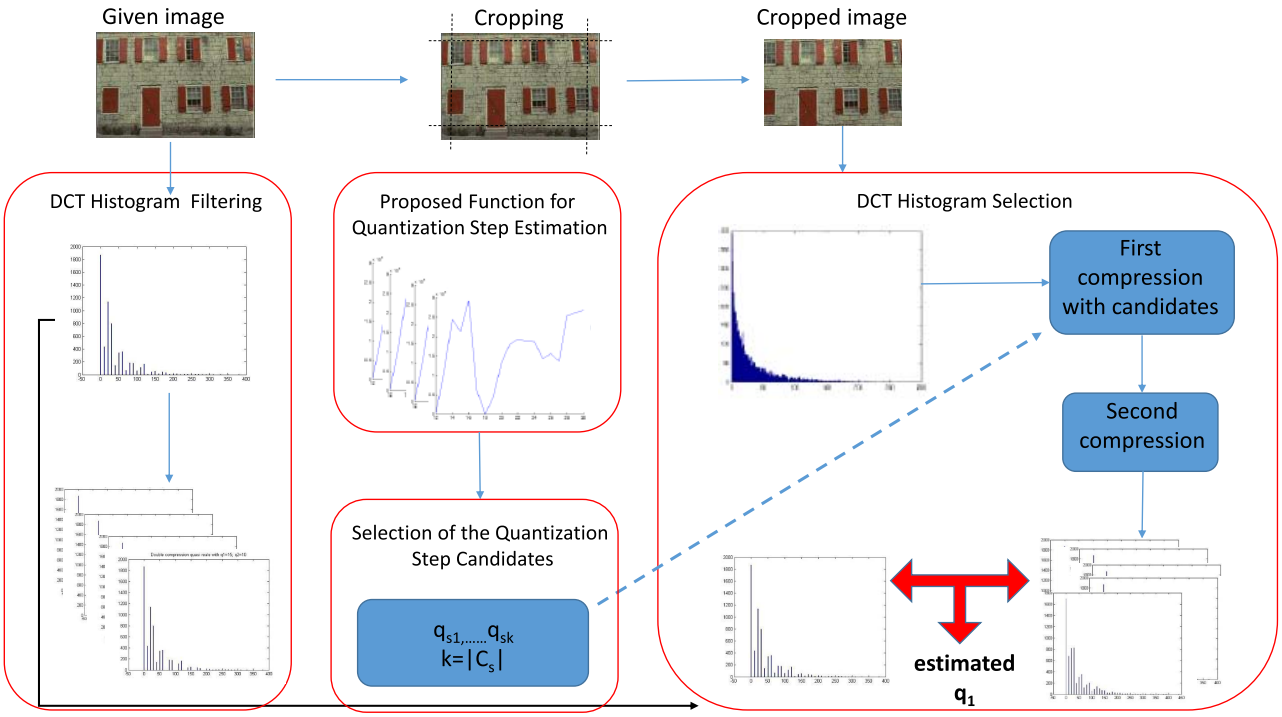

Fig. 2. Proposed approach scheme. Starting from an image I, exploiting the effects of successive quantizations, it estimates the quantization steps of the first quantization q_1. First, the histogram of the absolute value of DCT coefficients is filtered, then a proper function able to detect the first quantization step is evaluated and a set of candidates is selected. Later, considering the DCT coefficients related to a cropped version of the original image, the double quantization is simulated with the candidates previously computed. Finally, comparing the histogram of the original image with the simulated ones the first quantization step q_1 is estimated.

Obtaining a reliable q_1 estimation from Eq. (2) is a difficult task because too many cases have to be properly managed. In the following an alternative strategy devoted to increase the reliability of the estimation is proposed.

III. Proposed Approach

As described before, the function proposed in [25] is not able to work in real conditions. A first limit of Eq. (2) is related to its weak q_1 localization property. In real cases, many local minima are present in the function and localizing the correct one is a complex task. Another drawback of Eq. (2) is the neglecting of noise error e of Eq. (1). Considering then a real scenario, a method able to cope with the aforementioned problems has been built. Specifically, as shown in Fig. 2 the proposed approach consists of the following main steps:

- DCT Histogram Filtering: A deep analysis on the consequences of both quantization and rounding error has been performed. While indeed the former is well known, the rounding error e in Eq. (1) manifests itself as peaks spread around the multiples of the quantization step q, as exposed in [33] and has been modeled as an approximate Gaussian noise. As we will explain in more detail later, those joint phenomenons will affect the behavior of the second quantization step, thus the magnitude of the DCT coefficients, and consequently its statistics. For those reasons, the filtering strategy must face two kind of noise: the "split noise" and the "residual noise", with the aim to bring the histogram as if the rounding error did not have impact. This module actually provides a set of filtered histograms $H_{filt_{q_{1i}}}$ (one for each quantization step $q_{1i} \in \{q_{1min}, q_{1min}+1, \ldots, q_{1max}\}$).
- Proposed Function for Quantization Step Estimation: once the histogram has been filtered removing (or reducing) the error e, a function exploiting the properties of successive quantizations is needed. Specifically, a function with a q_1 localization property sensibly better than Eq. (2) has been designed. This function is actually evaluated over all the histograms $H_{filt_{q_{1i}}}$ generating a set of output $f_{out_{q_{1i}}}$.
- Selection of the Quantization Step Candidates: starting from the set of output $f_{out_{q_{1i}}}$, a limited number of first quantization candidates ($q_{1s} \in C_s$) are selected exploiting the q_1 localization property of the proposed error function.
- DCT Histogram Based Selection: the previous modules actually provide a series of q_1 candidates to be considered for further evaluations. The double quantization process is then simulated to consider the candidates provided by the other blocks and the best one exploiting directly histogram values is finally selected.

The above mentioned steps are detailed in the following subsections.

A. DCT Histogram Filtering

Many approaches exploiting the effects of successive quantizations followed by dequantizations ([13], [25], [27]) usually do not consider the error factor e in Eq. (1). This simplification allows to easily manipulate the involved equations, but

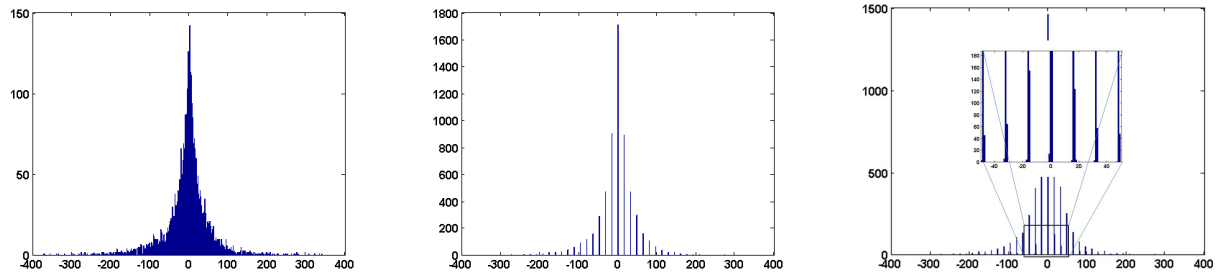

(a) (b) (c)

Fig. 3. DCT coefficient histograms during different stages of a double compression pipeline, referred to a specific position into the 8×8 image block: (a) histogram related to the original uncompressed image just after the DCT, (b) histogram related to the single compressed image, (c) histogram related to the DCT coefficients just before the second quantization (color conversions, rounding and truncation of the values to eight bit integers have been already performed). A detail was also overimposed for better visualization of the error e of Eq. (1).

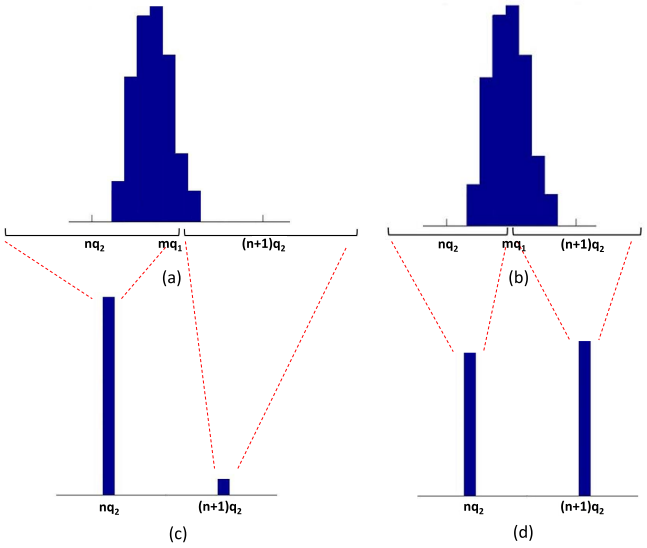

Fig. 4. Depending on the values of the first and the second quantization steps, different situations can arise. Specifically, the effect of the error e in the final histogram can be limited (c) or difficult to deal with (d).

neglecting this source of error considerably degrades the performances of these approaches when real cases are considered. To cope with this problem, a deep analysis of the properties of this source of error has been performed. As already explained before, it is introduced by several operations, such as color conversions (YCbCr to RGB and vice versa), rounding and truncation of the values to eight bit integers, etc. It is difficult to analyze each source of error separately, since it depends on the actual implementation, but the overall effect can be modeled with a Gaussian distribution ([22], [35]). An example of real DCT coefficient histograms is reported in Fig. 3.

The histogram depicted in Fig. 3(c) actually shows the DCT coefficient distribution just before the application of the second quantization. Once the image is compressed again, several scenarios can arise depending on the values of the first and second quantization steps. A typical scenario is the one reported in Fig. 4(a) and Fig. 4(c) where only a small perturbation (i.e., elements in a wrong bin) is propagated in the final histogram. On the contrary, in some specific conditions related to the q_1 and q_2 values a worst scenario can arise. As shown in Fig. 4(b) and Fig. 4(d) the original information can be quite equally split into two neighboring bins where one of them is a wrong one. This undesirable situation appears when a bin of the first quantization (i.e., in position mq_1) is situated exactly halfway between two consecutive bins coming from the second quantization (i.e., in position nq_2 and $(n+1)q_2$). Specifically, this effect arises when two consecutive multiples of q_2 are related to a generic multiple of q_1 as follows:

$$mq_1 = \frac{nq_2 + (n+1)q_2}{2}, \qquad n, m \in \mathbb{N}^+ \tag{3}$$

This behavior should be then taken into account in the design of algorithms aiming to exploit the effects of double quantizations. To properly cope with the noise e in Eq. (1) a filtering strategy has been developed. We have designed an approach based on two steps (see Fig. 5): the first one is devoted to filter the "split noise" (i.e., the one shown in Fig. 4(d)), whereas the second one deals with the residual noise (Fig. 4(c)).

Considering a specific pair of quantization steps q_1 and q_2 we design a filtering strategy that first detects the wrong bins on the second quantization histogram by using the Eq. (3) and then moves bin elements from the wrong to the correct ones. It is worth noting that the correct q_1 value is actually unknown and its estimation is the aim of the proposed approach. Several filtering are then performed considering a set of first quantization steps in the range $q_{1i} \in \{q_{1min}, q_{1min}+1, \ldots, q_{1max}\}$. The actual selection of the correct value will be performed later (see Section III-D) employing further analyses and tests.

Once the "split filter" has been performed, the residual noise is taken into account to remove further impurities (Fig. 3). Specifically, a filtering strategy based on the preservation of the monotonicity of the DCT coefficient distribution is employed (see Algorithm 1). As already reported in [36], AC coefficients are usually characterized by Laplace distribution. Initially, the histogram of absolute value of DCT coefficients is considered. Both bin index (i_{max}) and value (v_{max}) related to the maximum element of the histogram are then considered. All the values of the bins with index lower than i_{max} are compared with v_{max} and the ones below a certain relative threshold (Th_{filt}) are discarded. Once this filtering is performed, a novel interval of the histogram is

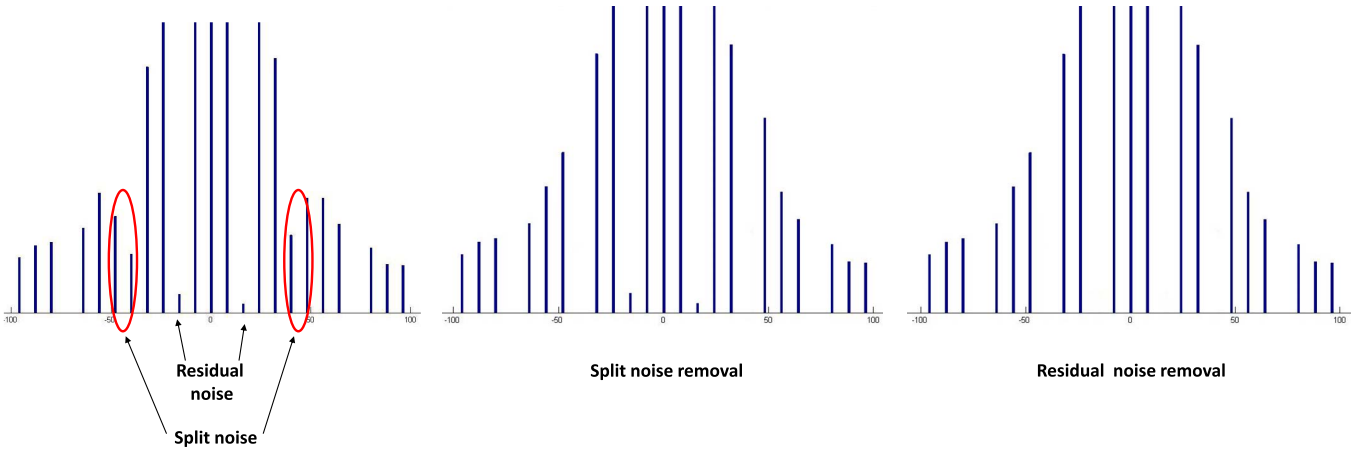

Fig. 5. Example of histogram filtering. First wrong bins on the second quantization histogram are detected by using the Eq. (3) and then they are moved to the correct locations. Later, the residual error is removed exploiting the monotonicity of the DCT coefficient distribution (see Algorithm 1).

Algorithm 1: AC Coefficients Histogram Filtering

Input:
H_{in}: input histogram of absolute values of DCT coefficients
N_{bins}: number of bins of H_{in}
Th_{filt}: threshold used to measure the similarity between bins
Output:
H_{filt}: filtered histogram
begin
  $H_{tmp} = H_{in}$
  $i_{max_{old}} = 1$
  while $i_{max_{old}} != N_{bins}$ **do**
    $[v_{max}, i_{max}] = max(H_{tmp})$
    for $i = i_{max_{old}} + 1$ ***to*** $i_{max} - 1$ **do**
      $v_{curr} = H_{in}[i]$
      if $v_{curr} > v_{max} \cdot Th_{filt}$ **then**
        $H_{filt}[i] = v_{curr}$
      else
        $H_{filt}[i] = 0$
      $H_{tmp}[i] = -1$
    $H_{tmp}[i_{max}] = -1$
    $H_{filt}[i_{max}] = H_{in}[i_{max}]$
    $i_{max_{old}} = i_{max}$
end

considered again and the same algorithm is applied (search of the maximum, filtering, etc.). This filtering works properly only for AC coefficients due to the monotonicity of their distribution. A different kind of filtering is then applied to DC coefficients. Specifically, all the values below an adaptive threshold (e.g., the mean value) are simply discarded.

Due to the "split filter", this filtering process provides to the following modules a series of filtered histograms $H_{filt_{q_{1i}}}$, one for each involved first quantization step $q_{1i} \in \{q_{1min}, q_{1min}+1, \ldots, q_{1max}\}$. Further details about the setting of the range of variation of q_{1i} will be provided in Section III-E.

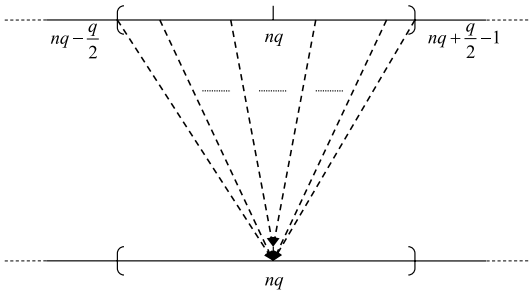

Fig. 6. The effect of quantization and dequantization for a generic term $c \in [nq - \frac{q}{2}, nq + \frac{q}{2} - 1]$ in case of q even.

B. Proposed Function for Quantization Step Estimation

As explained above, error function (2) has the following drawbacks: neglecting error e in Eq. (1) and a poor q_1 localization property. The former issue has been coped with the histogram filtering (see Section III-A) whereas the latter has been overcome by the design of the following error function:

$$f_{out}(c, q_1, q_2, q_3) = \left| \left[\left[\left[\left[\frac{c}{q_1} \right] \frac{q_1}{q_2} \right] \frac{q_2}{q_3} \right] \frac{q_3}{q_2} \right] q_2 - \left[\left[\frac{c}{q_1} \right] \frac{q_1}{q_2} \right] q_2 \right| \quad (4)$$

To properly understand the rationale of Eq. (4), especially when $q_3 = q_1$, it is sufficient to analyze the effect of a single quantization and dequantization step. If we examine the behavior of the following function:

$$\widehat{c} = \left[\frac{c}{q} \right] q \quad (5)$$

we can note that if q is odd, all integer numbers in $[nq - \lfloor \frac{q}{2} \rfloor, nq + \lfloor \frac{q}{2} \rfloor]$ will be mapped[2] in nq (with n a generic integer number). If q is even it maps in nq all the integer

[2] $\lfloor . \rfloor$ indicates the *floor* function.

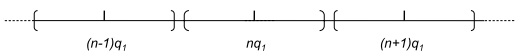

Fig. 7. The effect of quantization and dequantization for quantization step q_1.

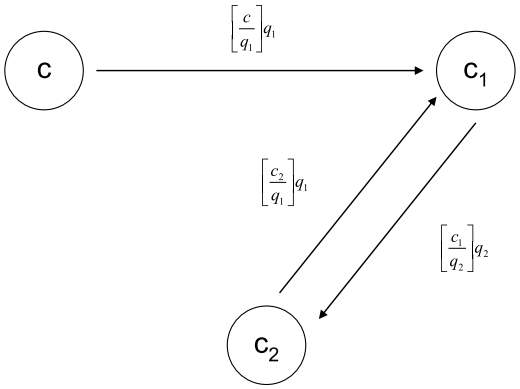

Fig. 8. Scheme describing the effect of three quantization and dequantization with quantization steps q_1, q_2 and $q_3 = q_1$ again.

numbers in $[nq - \frac{q}{2}, nq + \frac{q}{2} - 1]$. From now on we call this range "range related to nq". Such aspect is synthetically sketched in Fig. 6 (when q is even). As a consequence, we can say that Eq. (5) "groups" all integer numbers of its domain in multiples of q. Let observe that the maximum distance between a generic DCT coefficient c and the corresponding $\widehat{c}$, obtained by the quantization and dequantization process, is $\frac{q}{2}$ if q is even, $\lfloor \frac{q}{2} \rfloor$ if q is odd. Based on the above observation, we analyze three rounds applied in sequence, when $q_2 < q_1$ and $q_3 = q_1$:

$$\left[\left[\left[\frac{c}{q_1}\right]\frac{q_1}{q_2}\right]\frac{q_2}{q_1}\right]q_1 \tag{6}$$

- $c_1 = \left[\frac{c}{q_1}\right]q_1$ for the above observations leads to the situation shown in Fig. 7;
- $c_2 = \left[\frac{c_1}{q_2}\right]q_2$ maps multiples of q_1 in multiples of q_2. It is worth noting that, being $q_2 < q_1$, a generic nq_1 will be mapped in a multiple of q_2 (for example mq_2) whose distance from nq_1 will be less than or equal to $\frac{q_2}{2}$ (or $\lfloor \frac{q_2}{2} \rfloor$ if q_2 is odd), then in the range related to nq_1;
- at this point, $\left[\frac{c_2}{q_1}\right]q_1$ maps c_2 in nq_1 again, since, as pointed out in the preceding paragraph, c_2 is in the range related to nq_1.

With the three steps above, we demonstrated that (see Fig. 8):

$$\left[\left[\left[\frac{c}{q_1}\right]\frac{q_1}{q_2}\right]\frac{q_2}{q_1}\right]q_1 = \left[\frac{c}{q_1}\right]q_1 \tag{7}$$

Therefore the error function in (4) is 0 when $q_3 = q_1$ regardless the c value. This property allows then to localize the first quantization step with higher precision with respect to Eq. (2).

To sum up, this step, starting from the filtered histograms $H_{filt_{q_{1i}}}$, generates a set of function outputs $f_{out_{q_{1i}}}$.

C. Selection of the Quantization Step Candidates

As described in a previous subsection, due to the split filtering, the information related to the original histogram of a specific DCT frequency is tested considering different hypotheses related to the first quantization steps $q_{1i} \in \{q_{1min}, q_{1min} + 1, \ldots, q_{1max}\}$. Each function $f_{out_{q_{1i}}}$ is then related to a specific q_{1i} value. The main idea, allowing us selecting a limited set of first quantization candidates, is related to the properties of the proposed error function (4). Whenever the filtering is performed with the correct first quantization step, $f_{out_{q_{1i}}}$ is close to zero when $q_3 = q_{1i}$. On the contrary, when the first quantization is not the correct one, this property, usually, is not verified. This behavior allows to design a simple strategy of candidate selection. Specifically, considering a single DCT frequency, each $f_{out_{q_{1i}}}$ is evaluated in $q_3 = q_{1i}$ (where q_{1i} is the first quantization step related to the $f_{out_{q_{1i}}}$). If this value is close to zero (i.e., less than a threshold T), it is added to the set of candidates C_s otherwise it is discarded. The final estimation is then performed among the limited set exploiting directly the histogram values as detailed in the following section.

A crucial parameter that could impact the effectiveness of the proposed candidate selection strategy is the threshold T that determines the acceptance of the q_{1i} value. Choosing a low value, several correct elements could be lost (especially for higher DCT coefficients). On the other hand, higher values could include many false candidates that degrade the effectiveness of the overall strategy. Moreover, the value of $f_{out_{q_{1i}}}$ when $q_3 = q_{1i}$ depends on many factors such as the DCT frequency under examination and the actual content of the input image. To properly tune this parameter a series of tests has been then performed. A dataset containing 24 uncompressed images containing a certain variability in terms of scene content has been considered [31]. Double compression has been then performed by using standard JPEG encoding, and a dataset of double compressed images have been built just considering quality factors (QF_1, QF_2) in the range 50 to 100 at steps of 10. Taking into account the condition $q_1 > q_2$, the final dataset contains 360 images. Three different strategies have been compared:

- fixed threshold: a fixed threshold T_{fix} is selected without considering the dependency with respect to the frequency f_j and the content of the input histogram.
- first n: the values of $f_{out_{q_{1i}}}$ are sorted in increasing order. The n^{th} value is then retained as threshold.
- hybrid: the threshold is computed as the sum of the minimum value of $f_{out_{q_{1i}}}$ and a fixed threshold (T_{fix_h}).

Each strategy has been tested at varying of their involved parameters:

$$T_{fix} \in [100, 50000],\ n \in [1, 8],\ T_{fix_h} \in [100, 50000]$$

The percentage of first quantization steps correctly included into the candidate set has been plot with respect to the number of elements considered in the candidate set (see Fig. 9). These results have been obtained considering the average with respect to the image number and the considered frequencies (the first 15 DCT coefficients in zig-zag order in our test). As can be easily seen from Fig. 9 the hybrid approach provides

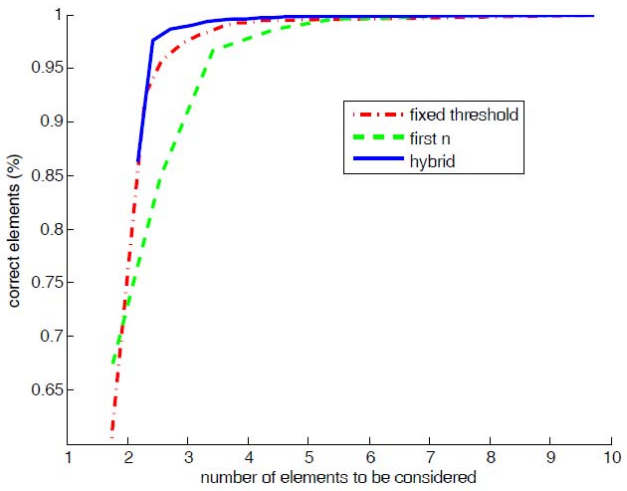

Fig. 9. Percentage of first quantization steps correctly included into the candidate set with respect to the number of elements in the candidate set. These results have been computed regarding the three considered strategies at varying of their parameters (T_{fix}; n; T_{fix_h}) and have been obtained as average over all frequencies (the first 15 DCT coefficients in zig-zag order) and treated images.

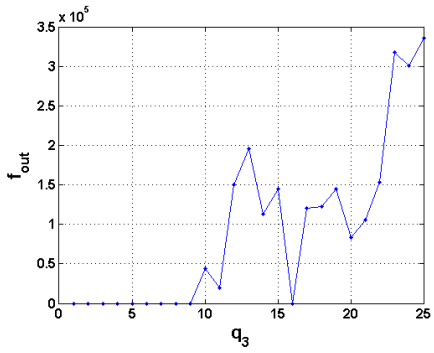

(a)

16	11	10	16	24	40	51	61
12	12	14	19	26	58	60	55
14	13	16	24	40	57	69	56
14	17	22	29	51	87	80	62
18	22	37	56	68	109	103	77
24	35	55	64	81	104	113	92
49	64	78	87	103	121	120	101
72	92	95	98	112	100	103	99

(b)

Fig. 10. Criteria for the selection of the range $\{q_{1min}, q_{1min}+1, \ldots, q_{1max}\}$: (a) error function (4) for an AC term in case of $q_1 = 16$, $q_2 = 9$ and $q_3 \in \{1, 2, \ldots, 25\}$. We can note that, for every $q_3 \leq q_2$, the result is 0. (b) The compression matrix for $QF = 50$, according with the original JPEG standard. The first 15 terms considering the order used in the entropy coding of the JPEG algorithm are underlined. The maximum expected compression step is 24.

the best performances. It is able to cope better than the other strategies with the content of the specific histogram.

D. DCT Histogram Selection

The modules presented above actually provide a series of first quantization candidates that have to be considered for further evaluations. The DCT Histogram Selection step, exploiting directly the information related to the histogram values estimates the q_1 value. In order to select the correct first quantization step, we exploit information coming from the original double compressed image I_{DQ}. We start with the extraction of DCT coefficients c_{DQ}, followed by a rough estimation of the original DCT coefficients obtained through a proper cropping of the double compressed image, as already proposed in [14]. These coefficients are then used as input of a double compression procedure, where the first quantization is performed by using $q_{1s} \in C_s$ whereas the second one using the already known values of the second quantization step (q_2 values are present in the header data). To estimate the correct q_1 from the candidate set, the whole histogram information is exploited. Specifically, the histograms $H_{q_{1s}}$ related to the simulated double quantization with $q_{1s} \in C_s$ are compared with H_{real} obtained from I_{DQ}. The closest one is selected according to the following criterion:

$$\widehat{q_1} = \min_{q_{1s} \in C_s} \sum_{i=1}^{N} \min(max_{diff}, |H_{real}(i) - H_{q_{1s}}(i)|) \quad (8)$$

where N is the number of bins of the histograms and max_{diff} is a threshold used to limit the contribution of a single difference in the overall distance computation.

E. Definition of the Range of Variability of q_3

To properly set the range of variability of the third quantization step the outcome of Eq. (4) should be better analyzed. Specifically, in case of $q_3 \leq q_2$, the proposed function is always equal to 0. Indeed in this situation, starting from bins located in multiples of q_2, $\left[\frac{c_2}{q_3}\right] q_3$ will drive the bins in multiples of q_3 that belong to the range related to nq_2. For this reason, the fourth quantization step with $q = q_2$ will drive again the bins in multiples of q_2. In Fig. 10(a) we can see an example of the behavior of Eq. (4) in case of $q_1 = 16$ and $q_2 = 9$. For this reason, we always consider $q_2 + 1$ as the term q_{1min}.

The compression matrix defined by the IJG [32] for the quality factor 50 (the lower one considered in this work, i.e., the matrix with the higher quantization steps for every position) is the one showed in Fig. 10(b). Since we extended our study to its first 15 positions following the zig-zag order used in the JPEG algorithm during the entropy coding, the higher quantization step (in position (0,4)) is 24. For this reason, and considering the need to visualize also the trend after this value, we set q_{1max} to 30.

IV. Experimental Results

To assess the performance of the proposed approach, several tests have been conducted considering double compressed JPEG images, obtained starting from two different sources as described below. A dataset of 110 uncompressed images has been collected considering different cameras (Canon D40, Canon D50 e Canon Mark3) with different resolutions.

TABLE I

PERCENTAGE OF ERRONEOUSLY ESTIMATED q_1 VALUES AT VARYING OF QUALITY FACTOR (QF_1, QF_2) RELATIVE TO THE FIRST 15 DCT COEFFICIENTS IN ZIG-ZAG ORDER. EVERY COEFFICIENT IS INDICATED WITH RESPECT TO ITS POSITION IN THE 8×8 IMAGE BLOCK.(0,0) IS THE DC TERM

(0,0)

QF_1 \ QF_2	60	70	80	90	100
50	0,00%	0,00%	0,00%	0,00%	0,00%
60		0,91%	0,00%	0,00%	0,00%
70			0,91%	0,00%	0,91%
80				0,00%	0,00%
90					0,00%

(1,0)

QF1 \ QF_2	60	70	80	90	100
50	0,00%	0,00%	0,00%	0,00%	0,00%
60		0,00%	0,00%	0,00%	0,00%
70			0,00%	0,00%	0,00%
80				0,00%	0,00%
90					0,00%

(2,0)

QF_1 \ QF_2	60	70	80	90	100
50	0,00%	0,00%	0,00%	0,00%	0,00%
60		1,82%	0,00%	0,00%	0,00%
70			0,00%	0,00%	0,00%
80				0,00%	0,00%
90					0,00%

(3,0)

QF_1 \ QF_2	60	70	80	90	100
50	1,82%	1,82%	0,00%	0,00%	0,00%
60		1,82%	1,82%	0,00%	0,00%
70			0,00%	0,00%	0,00%
80				0,00%	0,00%
90					0,00%

(4,0)

QF_1 \ QF_2	60	70	80	90	100
50	0,00%	0,00%	0,91%	0,00%	0,00%
60		0,00%	0,00%	0,00%	0,00%
70			0,00%	0,00%	0,00%
80				0,00%	0,00%
90					0,00%

(0,1)

QF_1 \ QF_2	60	70	80	90	100
50	0,00%	0,00%	0,00%	0,00%	0,91%
60		0,91%	0,00%	0,00%	0,00%
70			0,91%	0,00%	0,00%
80				0,00%	0,00%
90					0,00%

(1,1)

QF_1 \ QF_2	60	70	80	90	100
50	12,73%	16,36%	0,91%	0,00%	0,00%
60		1,82%	1,82%	0,00%	0,00%
70			0,00%	0,00%	0,00%
80				0,00%	0,00%
90					0,00%

(2,1)

QF_1 \ QF_2	60	70	80	90	100
50	2,73%	4,55%	0,00%	0,00%	0,00%
60		0,91%	0,91%	0,00%	0,00%
70			0,00%	0,00%	0,00%
80				0,00%	0,00%
90					0,00%

(3,1)

QF_1 \ QF_2	60	70	80	90	100
50	0,91%	0,91%	0,00%	0,91%	0,00%
60		0,91%	0,00%	0,00%	0,00%
70			0,00%	0,00%	0,00%
80				0,00%	0,00%
90					0,00%

(0,2)

QF_1 \ QF_2	60	70	80	90	100
50	3,64%	5,45%	0,00%	0,91%	0,00%
60		3,64%	2,73%	0,00%	0,00%
70			0,00%	0,00%	0,00%
80				0,00%	0,00%
90					0,00%

(1,2)

QF_1 \ QF_2	60	70	80	90	100
50	10,91%	58,18%	15,45%	3,64%	0,00%
60		6,36%	25,45%	0,91%	0,00%
70			10,00%	0,91%	0,00%
80				0,00%	0,00%
90					0,00%

(2,2)

QF_1 \ QF_2	60	70	80	90	100
50	14,55%	2,73%	54,55%	0,00%	0,00%
60		16,36%	10,91%	0,91%	0,00%
70			18,18%	0,00%	0,00%
80				0,00%	0,00%
90					0,00%

(0,3)

QF_1 \ QF_2	60	70	80	90	100
50	20,00%	22,73%	0,00%	3,64%	0,91%
60		1,82%	8,18%	1,82%	0,00%
70			0,00%	0,00%	0,00%
80				0,00%	0,00%
90					0,00%

(1,3)

QF_1 \ QF_2	60	70	80	90	100
50	12,73%	9,09%	19,09%	4,55%	0,00%
60		47,27%	7,27%	1,82%	0,00%
70			1,82%	1,82%	0,00%
80				0,00%	0,00%
90					0,00%

(0,4)

QF_1 \ QF_2	60	70	80	90	100
50	20,91%	16,36%	20,00%	13,64%	0,91%
60		50,00%	47,27%	10,00%	0,00%
70			4,55%	6,36%	0,00%
80				0,91%	0,00%
90					0,00%

Moreover, a certain variability in terms of image content has been taken into account in the image acquisition. The considered dataset (Canon D40D50MK3 Dataset from here on) contains: people, landscapes, coasts, mountains, animals, flowers, buildings, foods, bridges, trees, etc. A cropping of size 1024×1024 of the central part of each image has been then selected in order to speed up the tests. Starting from the cropped images, applying JPEG encoding provided by Matlab with standard JPEG quantization tables proposed by IJG (Independent JPEG Group) [37], a dataset of double compressed images have been built just considering quality factors (QF_1, QF_2) in the range 50 to 100 at steps of 10. Taking into account the condition $q_1 > q_2$ (i.e., $QF_2 > QF_1$ in our tests), the final dataset contains 1650 images. It is worth noting that this experimental methodology (i.e., testing the performance of the algorithm at varying of the quality factors) has been applied in many works related to double quantization problem ([14], [20], [22], [25], [27], [28]). Results are then reported with respect to quality factors instead of the specific quantization steps. This methodology simplifies the analysis of the results, since a single parameter (quality factor) describes a quantization matrix with 64 quantization steps usually having different values and related to different frequencies. As an example, the quantization matrix for $QF = 50$ is reported in Fig. 10(b).

Table I reports the average percentage of erroneously estimated q_1 values at varying of quality factor, relative to the first 15 DCT coefficients considered in zig-zag order. This order, used in the standard JPEG, allows sorting the coefficients from the lowest frequency (DC) to the highest frequencies in a 1D vector. The estimation error of the proposed approach is close to zero for the DCT coefficients related to low frequency in the DCT domain and does not significantly depend on the specific quality factor employed for the first and second

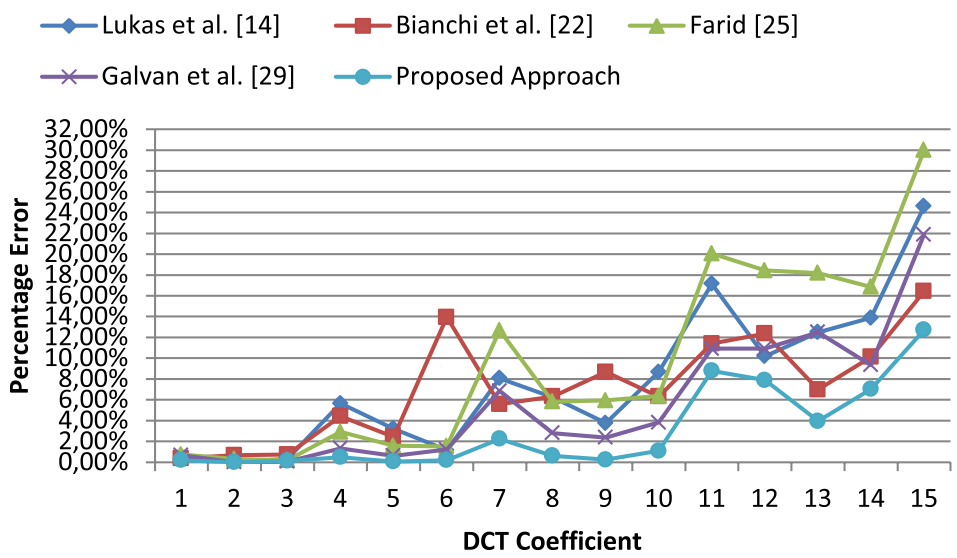

Fig. 11. Percentage of erroneously estimated q_1 values at varying of DCT coefficient position (zig-zag scanning) considering several state-of-the-art approaches on the Canon D40D50MK3 Dataset. These values are obtained averaging over all (QF_1,QF_2) and images.

quantization. On the contrary, for higher frequencies, the estimation error is strictly correlated with the quality factors. Specifically, better results are usually obtained for higher QF_1 and QF_2 values corresponding to lower quantization.

Further analyses have been conducted in order to study the performance of the proposed approach with respect to the specific DCT coefficient. In Fig. 11 the percentage error in the estimation of q_1, at varying of the DCT coefficients from low to high frequencies, is reported. These errors are average values obtained considering all the combinations of (QF_1, QF_2) indicated in table I. As expected the performance of the proposed solution degrades with DCT coefficients corresponding to the highest frequencies. The proposed approach estimates with high accuracy the first 10 coefficients with an error usually lower than 2%. The estimation of the other DCT coefficients (higher than 10^{th}) is actually reliable only considering high QF_2 values. It is worth noting that the results related to some frequencies (4^{th}, 7^{th}, 11^{th}) seem to differ with respect to the trend of the curve error. This behavior depends on the cropping procedure employed in the DCT Histogram Selection step (see Section III-D). First quantization actually introduces blocking artifacts, especially if lower quality factor are employed, between blocks that cannot be removed by simple cropping and influences the frequency content of the image. Specifically, the frequencies of positions 4^{th}, 7^{th}, 11^{th} are related to horizontal and vertical edges and are pretty sensitive to the aforementioned kind of artifacts.

The method has been compared with the algorithms proposed in [14], [22], and [29]. Specifically, the original code (available online) related to Bianchi et al. [22], has been considered whereas the method based on the direct comparison of histograms described in [14] has been reimplemented. Finally, to further validate the effectiveness of the proposed function (4), the approach proposed in [29] has been considered by using Eq. (2) proposed in [25] instead of Eq. (4). All techniques have been tested considering the first quantization step in the range $[1, 30]$. Moreover, the following parameter setting has been used: histogram filtering $Th_{filt} = 0.35$ (see Section III-A), hybrid strategy with $T_{fix_h} = 5000$ for AC coefficients and $T_{fix_h} = 100000$ for DC coefficient (see Section III-C), $max_{diff} = 100$ (see Section III-D). The cropping has been performed by removing both the first and the last 4 rows and columns. It is worth noting that all the parameter settings related to the proposed approach have been performed on the dataset [36].

As already underlined in Section II, the function proposed in [25] has a poor q_1 localization property that degrades its performances. Moreover, the filtering step (see Section III-A) allows to considerably improve the performances of the proposed approach with respect to method in [29] that do not cope with error e in Eq. (1). The direct histogram comparison proposed in [14], without any filtering and candidate selection, is not able to deal with the low quality data related to higher frequencies. Although Bianchi et al. [22] consider in their model the noise e of Eq. (1) they actually do not perform any kind of filtering. The combination of a filtering strategy with a function having a good q_1-localization property, allows us outperforming the other state-of-the-art approaches (see Fig. 11) both for low and high frequencies.

To further confirm the effectiveness of the proposed approach, additional tests have been performed on the standard dataset "Uncompressed Colour Image Database" (UCID) [38]. Specifically, the UCID (v2) contains 1338 uncompressed TIFF images with a certain variability in terms of scene content (natural, man-made objects, indoor, outdoor, etc.). Moreover, image sizes are 512×384 or 384×512. A novel compressed dataset has then been built, with the same methodology explained before: quality factors (QF_1, QF_2) in the range 50 to 100 at steps of 10 and $q_1 > q_2$. The final dataset contains 20070 double compressed images.

As can be easily seen from Fig. 12, the proposed solution outperforms, almost everywhere, the state-of-the-art approaches. It is worth noting that the performances of the considered methods in this test are lower than the ones

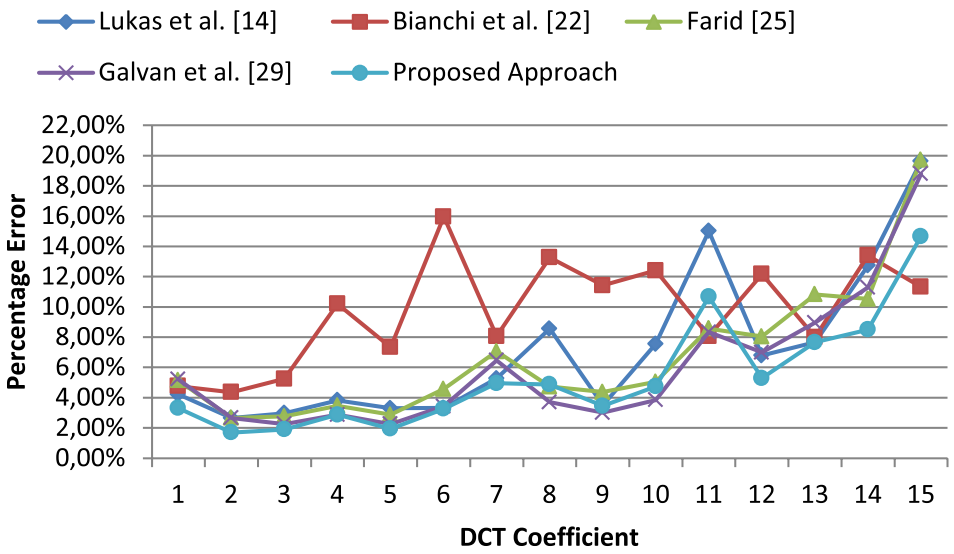

Fig. 12. Percentage of erroneously estimated q_1 values at varying of DCT coefficient position (zig-zag scanning) considering several state-of-the-art approaches on the UCID (v2) dataset. These values are obtained averaging over all (QF_1, QF_2) and images.

shown in Fig. 11. Indeed, the outcomes of the considered approaches depend on the resolution of the image under analysis. If the image size is low, few JPEG blocks can be collected and the reliability of the analysis could be low. In the first test, performed on the Canon D40D50MK3 Dataset, 16384 JPEG blocks are collected per image, whereas in the UCID (v2) Dataset the number of blocks was only 3072. However, working with small images is not the common scenario, and also nowadays images have bigger resolution compared to the ones used in our tests. Moreover, in a tampering scenario in which a patch is pasted over a portion of the original image, the above considerations are still valid. The unmodified regions will undergo to a double compression and, even if the pasted part is significantly smaller compared to the image, the number of available blocks to perform a correct estimation can be enough.

V. Conclusion

In this paper we proposed a novel algorithm for the estimation of the first quantization steps from double compressed JPEG images. The proposed approach, combining a filtering strategy and an error function with a good q_1-localization property, obtains satisfactory results outperforming the other state-of-the-art approaches both for low and high frequencies. Future works will be devoted to cope with the case when $q_1 < q_2$, and to exploit the proposed approach to recover the overall initial quantization matrix considering a double compression process achieved by applying actual quantization tables used by camera devices and common photo-retouching software (e.g., Photoshop, Gimp, etc.).

Acknowledgment

We thank AMPED SRL [39] for providing us useful code for DCT coefficient manipulation.

References

[1] (2014). *Usage of Image File Formats for Websites* [Online]. Available: http://w3techs.com/technologies/overview/image_format/all

[2] E. Kee, M. K. Johnson, and H. Farid, "Digital image authentication from JPEG headers," *IEEE Trans. Inf. Forensics Security*, vol. 6, no. 3, pp. 1066–1075, Sep. 2011.

[3] A. Piva, "An overview on image forensics," in *Proc. ISRN Signal Process.*, 2013, p. 496701.

[4] M. C. Stamm, M. Wu, and K. J. R. Liu, "Information forensics: An overview of the first decade," *IEEE Access*, vol. 1, pp. 167–200, May 2013.

[5] A. R. Bruna, G. Messina, and S. Battiato, "Crop detection through blocking artefacts analysis," in *Proc. Int. Conf. Image Anal. Process. (ICIAP)*, vol. 6978. Sep. 2011, pp. 650–659.

[6] W. Luo, Z. Qu, J. Huang, and G. Qiu, "A novel method for detecting cropped and recompressed image block," in *Proc. IEEE Int. Conf. Acoust., Speech Signal Process. (ICASSP)*, vol. 2. Apr. 2007, pp. II–217–II–220.

[7] S. Battiato, G. M. Farinella, E. Messina, and G. Puglisi, "Robust image alignment for tampering detection," *IEEE Trans. Inf. Forensics Security*, vol. 7, no. 4, pp. 1105–1117, Aug. 2012.

[8] E. Kee and H. Farid, "Digital image authentication from thumbnails," in *Proc. SPIE*, vol. 7541. Jan. 2010.

[9] T. Gloe, "Forensic analysis of ordered data structures on the example of JPEG files," in *Proc. IEEE Int. Workshop Inform. Forensics Security (WIFS)*, 2012, pp. 139–144.

[10] Y. Chen and V. L. L. Thing, "A study on the photo response non-uniformity noise pattern based image forensics in real-world applications," in *Proc. Int. Conf. Image Process., Comput. Vis., Pattern Recognit. (IPCV)*, Jul. 2012.

[11] S. Battiato and G. Messina, "Digital forgery estimation into DCT domain: A critical analysis," in *Proc. ACM Workshop Multimedia Forensics (MiFor)*, 2009, pp. 37–42.

[12] J. A. Redi, W. Taktak, and J. L. Dugelay, "Digital image forensics: A booklet for beginners," *Multimedia Tools Appl.*, vol. 51, no. 1, pp. 133–162, Jan. 2011.

[13] A. C. Popescu and H. Farid, "Statistical tools for digital forensics," in *Proc. 6th Int. Workshop Inform. Hiding*, May 2004, pp. 128–147.

[14] J. Lukas and J. Fridrich, "Estimation of primary quantization matrix in double compressed JPEG images," in *Proc. Digit. Forensic Res. Workshop (DFRWS)*, 2003, pp. 5–8.

[15] J. He, Z. Lin, L. Wang, and X. Tang, "Detecting doctored JPEG images via DCT coefficient analysis," in *Proc. 9th Eur. Conf. Comput. Vis. (ECCV)*, vol. 3953. May 2006, pp. 423–435.

[16] C. Chen, Y. Q. Shi, and W. Su, "A machine learning based scheme for double JPEG compression detection," in *Proc. 19th Int. Conf. Pattern Recognit. (ICPR)*, Dec. 2008, pp. 1–4.

[17] V. L. L. Thing, Y. Chen, and C. Cheh, "An improved double compression detection method for JPEG image forensics," in *Proc. IEEE Int. Symp. Multimedia (ISM)*, Dec. 2012, pp. 290–297.

[18] F. Huang, J. Huang, and Y. Q. Shi, "Detecting double JPEG compression with the same quantization matrix," *IEEE Trans. Inf. Forensics Security*, vol. 5, no. 4, pp. 848–856, Dec. 2010.

[19] Q. Liu, "Detection of misaligned cropping and recompression with the same quantization matrix and relevant forgery," in *Proc. 3rd Int. ACM Workshop Multimedia Forensics Intell. (MiFor)*, 2011, pp. 25–30.
[20] T. Pevny and J. Fridrich, "Detection of double-compression in JPEG images for applications in steganography," *IEEE Trans. Inf. Forensics Security*, vol. 3, no. 2, pp. 247–258, Jun. 2008.
[21] W. Wang, J. Dong, and T. Tan, "Exploring DCT coefficient quantization effect for image tampering localization," in *Proc. IEEE Int. Workshop Inform. Forensics Security (WIFS)*, Nov./Dec. 2011, pp. 1–6.
[22] T. Bianchi and A. Piva, "Image forgery localization via block-grained analysis of JPEG artifacts," *IEEE Trans. Inf. Forensics Security*, vol. 7, no. 3, pp. 1003–1017, Jun. 2012.
[23] R. N. Neelamani, R. de Queiroz, Z. Fan, and R. G. Baraniuk, "JPEG compression history estimation for color images," *IEEE Trans. Image Process.*, vol. 15, no. 6, pp. 1365–1378, Jun. 2006.
[24] T. Gloe, "Demystifying histograms of multi-quantised DCT coefficients," in *Proc. IEEE Int. Conf. Multimedia Expo (ICME)*, Jul. 2011, pp. 1–6.
[25] H. Farid, "Exposing digital forgeries from JPEG ghosts," *IEEE Trans. Inf. Forensics Security*, vol. 1, no. 4, pp. 154–160, Mar. 2009.
[26] F. Zach, C. Riess, and E. Angelopoulou, "Automated image forgery detection through classification of JPEG ghosts," in *Proc. Joint 34th German Assoc. Pattern Recognit. (DAGM), 36th Austrian Assoc. Pattern Recognit. (OAGM) Symp.*, vol. 7476. Aug. 2012, pp. 185–194.
[27] Z. Lin, J. He, X. Tang, and C.-K. Tang, "Fast, automatic and fine-grained tampered JPEG image detection via DCT coefficient analysis," *Pattern Recognit.*, vol. 42, no. 11, pp. 2492–2501, Nov. 2009.
[28] T. Bianchi, A. D. Rosa, and A. Piva, "Improved DCT coefficient analysis for forgery localization in JPEG images," in *Proc. IEEE Int. Conf. Acoust., Speech, Signal Process. (ICASSP)*, May 2011, pp. 2444–2447.
[29] F. Galvan, G. Puglisi, A. R. Bruna, and S. Battiato, "First quantization coefficient extraction from double compressed JPEG images," in *Proc. 17th Int. Conf. Image Anal. Process. (ICIAP)*, vol. 8156. Sep. 2013, pp. 783–792.
[30] G. Puglisi, A. R. Bruna, F. Galvan, and S. Battiato, "First JPEG quantization matrix estimation based on histogram analysis," in *Proc. 20th IEEE Int. Conf. Image Process. (ICIP)*, Sep. 2013, pp. 4502–4506.
[31] G. K. Wallace, "The JPEG still picture compression standard," *Commun. ACM*, vol. 34, no. 4, pp. 30–44, Apr. 1991.
[32] S. Battiato, M. Mancuso, A. Bosco, and M. Guarnera, "Psychovisual and statistical optimization of quantization tables for DCT compression engines," in *Proc. 11th Int. Conf. Image Anal. Process. (ICIAP)*, Sep. 2001, pp. 602–606.
[33] W. Luo, J. Huang, and G. Qiu, "JPEG error analysis and its applications to digital image forensics," *IEEE Trans. Inf. Forensics Security*, vol. 5, no. 3, pp. 480–491, Sep. 2010.
[34] Z. Fan and R. L. de Queiroz, "Identification of bitmap compression history: JPEG detection and quantizer estimation," *IEEE Trans. Image Process.*, vol. 12, no. 2, pp. 230–235, Feb. 2003.
[35] E. Y. Lam and J. W. Goodman, "A mathematical analysis of the DCT coefficient distributions for images," *IEEE Trans. Image Process.*, vol. 9, no. 10, pp. 1661–1666, Oct. 2000.
[36] (2014). *Dataset Eastman Kodak* [Online]. Available: http://r0k.us/graphics/kodak/
[37] (2014). *Independent JPEG Group* [Online]. Available: http://www.ijg.org/
[38] G. Schaefer and M. Stich, "UCID-an uncompressed colour image database," in *Proc. SPIE*, vol. 5307, 2004, pp. 472–480.
[39] (2014). *Amped Software*. Amped SRL, Trieste, Italy [Online]. Available: http://ampedsoftware.com/company

Fausto Galvan was born in Belluno, Italy, in 1969. He received the degree in mathematics from the University of Udine, Udine, Italy, in 2002, where he is currently pursuing the Ph.D. degree in computer science with the Department of Mathematics and Computer Science. His current research interest is image/video forensics. In 1991, he joined the Carabinieri Police Force.

Giovanni Puglisi was born in Acireale, Italy, in 1980. He received the M.S. (*summa cum laude*) degree in computer science engineering and the Ph.D. degree in computer science from Catania University, Catania, Italy, in 2005 and 2009, respectively. He is currently a contract Researcher with the Department of Mathematics and Computer Science, Catania University. His research interests include image/video enhancement and processing, camera imaging technology, and multimedia forensics. He has edited one book, and co-authored more than 40 papers in international journals, conference proceedings, and book chapters. He is a co-inventor of several patents, and serves as a reviewer of different international journals and conferences.

Arcangelo Ranieri Bruna received the Italian degree in electronic engineer from the University of Palermo, Palermo, Italy, in 1998, and the Ph.D. degree in applied mathematics from the University of Catania, Catania, Italy. He was with a telecommunication firm in Rome. He then joined STMicroelectronics, Catania, in 1999, where he is with the Advanced System Technology Catania Laboratory. His current research interests are in the areas of digital image processing from the physical digital acquisition to the final image compression, computer vision, and image forensics. He has authored several papers and book chapters, and holds several international patents on these activities.

Sebastiano Battiato (M'04–SM'06) received the degree in computer science (*summa cum laude*) from the University of Catania, Catania, in 1995, and the Ph.D. degree in computer science and applied mathematics from the University of Naples, Naples, Italy, in 1999. From 1999 to 2003, he was the leader of the Imaging Team at STMicroelectronics, Catania. He joined the Department of Mathematics and Computer Science at the University of Catania as an Assistant Professor in 2004, and became an Associate Professor in 2011. His research interests include image enhancement and processing, image coding, camera imaging technology, and multimedia forensics. He has edited six books and coauthored more than 150 papers in international journals, conference proceedings, and book chapters. He is a co-inventor of about 15 international patents, a reviewer for several international journals, and he has been regularly a member of numerous international conference committees. He has participated in many international and national research projects. He was the Chair of several international events (the International Workshop on Computer Vision in 2012, the European Conference on Computer Vision in 2012, the International Conference on Computer Vision Theory and Applications from 2012 to 2014, the International Conference on Image Analysis and Processing in 2011, the International ACM Workshop on Multimedia in Forensics and Intelligence from 2010 to 2011, and the SPIE EI Digital Photography from 2011 to 2013). He is an Associate Editor of the IEEE TRANSACTIONS ON CIRCUITS AND SYSTEM FOR VIDEO TECHNOLOGY and the *SPIE Journal of Electronic Imaging*, a Guest Editor of the following special issues, Emerging Methods for Color Image and Video Quality Enhancement published in *EURASIP Journal on Image and Video Processing* (2010) and Multimedia in Forensics, Security and Intelligence published in the *IEEE Multimedia Magazine* (2012). He was a recipient of the 2011 Best Associate Editor Award of the IEEE TRANSACTIONS ON CIRCUITS AND SYSTEMS FOR VIDEO TECHNOLOGY. He is the Director (and Co-Founder) of the International Computer Vision Summer School, Sicily, Italy.